

Transient kinetics of light-induced metastable states in single crystals and aqueous solutions of $\text{Na}_2[\text{Fe}(\text{CN})_5\text{NO}]\cdot 2\text{H}_2\text{O}$

D. Schaniel* and Th. Woike

Institut für Mineralogie, Universität zu Köln, Zùlpicherstrasse 49b, 50674 Köln, Germany

C. Merschjann and M. Imlau

Fachbereich Physik, Universität Osnabrück, Barbarastrasse 7, 49069 Osnabrück, Germany

(Received 18 August 2005; published 30 November 2005)

The generation and relaxation of light-induced metastable states at room temperature is investigated in single crystals and aqueous solutions of $\text{Na}_2[\text{Fe}(\text{CN})_5\text{NO}]\cdot 2\text{H}_2\text{O}$ (SNP), using transient absorption spectroscopy. The temporal monoexponential decay after exposure to nanosecond laser pulses results from the thermal deexcitation of the metastable state named SII. The lifetime τ of SII at $T=302$ K is $\tau=1.8(1)\times 10^{-7}$ s in single crystals and $\tau=1.1(1)\times 10^{-7}$ s in aqueous solutions. An Arrhenius-like behavior is verified yielding the activation energy $E_A=0.43(3)$ eV and the frequency factor $Z=7\times 10^{13}$ s $^{-1}$. The buildup time of the metastable state SII is faster than 1 ns and occurs via a singlet excited state. With an exposure of 0.8 J/cm 2 , 0.8(2)% of the molecules can be transferred from the ground state to SII.

DOI: [10.1103/PhysRevB.72.195119](https://doi.org/10.1103/PhysRevB.72.195119)

PACS number(s): 78.47.+p, 33.15.Hp, 64.60.My

I. INTRODUCTION

Optically generated metastable states are comprehensively investigated in photocrystallography under a variety of fundamental and technological aspects. Beside their amazing potential for photonic applications, such as optical switching or data storage,^{1,2} their biological function is of fundamental importance, especially for complexes containing nitric oxide (NO) as a ligand. Due to the well-known activity of the NO molecule in a wide range of important biological functions like neurotransmission, penile erection, enzyme-, immune- and blood pressure regulation, and even inhibition of tumor growth,³⁻⁷ a neutral carrier is needed in order to transport the NO to the desired position in the organism, where it should be released concertedly. Here the metastable states play an essential role, as the binding energy of the NO ligand is reduced by light irradiation.⁸

Up to now investigations in nitrosyl compounds are performed using frozen metastable states at sufficiently low temperatures allowing to apply time-consuming methods for characterization, such as Mössbauer,^{9,10} Raman- and infrared spectroscopy,¹¹⁻¹³ differential scanning calorimetry (DSC),^{14,15} absorption spectroscopy,¹⁶ holography,¹⁷ or even structural clarification by x-ray and neutron diffraction.¹⁸⁻²¹

Two metastable states named SI and SII, lying energetically 1–2 eV above the ground state (GS), are established in a variety of nitrosyl compounds of the general composition $X_n[\text{ML}_5\text{NO}]\cdot y\text{H}_2\text{O}$, in which the relevant NO ligand is bound to the central atom $M=\text{Fe}$, Ru, Os, etc. with different ligands $L=\text{F}$, Cl, Br, I, OH, CN, NH_3 , C_2O_4 , ethylenediamine, etc. and counter ions $X_n=\text{alkali}$, earth alkali, halogene, NH_4 , CN_3H_6 , etc., and different amounts of crystal water y .^{14,22,23} The highest decay temperature T_M (= peak in heat flow of the DSC curve) up to now is found in *trans*- $[\text{Ru}(\text{H}_2\text{O})(\text{NH}_3)_4\text{NO}]\text{Cl}_3\cdot \text{H}_2\text{O}$ with $T_M(\text{SI})=293$ K and $T_M(\text{SII})=225$ K.⁸ The photogeneration of both states is performed by irradiation with light in the violet-blue-green

spectral range below the decay temperature of SII. The metastable state SII corresponds to a *side-on* configuration of NO,^{18,20} where the NO-ligand is rotated by about 90° from the almost linear *M-N-O* ground state configuration. Inspired by the linkage isomer structure of SII it was suggested, based on the analysis of x-ray diffraction data, that SI corresponds to an *isonitrosyl M-O-N* configuration,¹⁸ an interpretation which is supported by calculations based on density functional theory (DFT).²⁴ However, a recent neutron diffraction study could not confirm this finding.¹⁹ The activation energies are 0.69 eV for SI and 0.46 eV for SII in $\text{Na}_2[\text{Fe}(\text{CN})_5\text{NO}]\cdot 2\text{H}_2\text{O}$ (sodium nitroprusside, SNP).¹⁵ With respect to the biological and technical applications, it is important to know the transient kinetics of the metastable states at room temperature. Especially the knowledge of the number density of metastable molecules generated with short light pulses is a necessary prerequisite for possible applications. We investigate the transient kinetics of the metastable states in $\text{Na}_2[\text{Fe}(\text{CN})_5\text{NO}]\cdot 2\text{H}_2\text{O}$ after optical generation with nanosecond laser pulses at room temperature using transient absorption spectroscopy. We demonstrate the existence of the light-induced metastable state SII even at room temperature and attribute its monoexponential decay to a thermally driven decay, whereby the 0.43 eV potential barrier is overcome. Furthermore we show that the generation of SII is also possible in aqueous solutions of SNP using nanosecond laser pulses.

II. EXPERIMENTAL DETAILS

The orthorhombic SNP single crystals (space group *Pnmm*) were cut perpendicular to the crystallographic axes and ground to thicknesses between 100 and 200 μm in view of the small penetration depth $1/\alpha=125$ μm ($\mathbf{E}\parallel c$ axis) of the pump pulses at 532 nm. The oriented single crystals are mounted on a sample holder with an aperture of 5 mm diameter, defining the illuminated area of $A=0.196$ cm 2 , per-

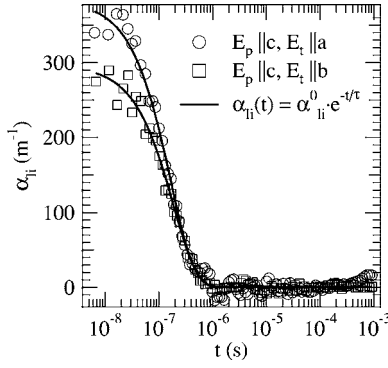


FIG. 1. Monoexponential decay of the light-induced absorption after pulsed illumination [$Q=0.12(1) \text{ J/cm}^2$] with $\lambda_p=532 \text{ nm}$ at room temperature for different polarizations of the probe beam ($\lambda_t=633 \text{ nm}$). \circ $\mathbf{E}_t \parallel a$: $\tau_a=1.7(1) \times 10^{-7} \text{ s}$, $\alpha_{li}^0=382(5) \text{ m}^{-1}$, $d=115 \mu\text{m}$. \square $\mathbf{E}_t \parallel b$: $\tau_b=1.9(1) \times 10^{-7} \text{ s}$, $\alpha_{li}^0=296(5) \text{ m}^{-1}$, $d=130 \mu\text{m}$.

pendicular to the incident pulsed light beam. Likewise the solutions, filled into optical cuvettes of thickness 1 mm and 2 mm, are mounted on the same sample holder. The laser pulses are produced using a frequency-doubled Q-switched Nd:YAG laser [Coherent Infinity: wavelength of 532 nm, pulse width of 4 ns, maximum energy of 250 mJ/pulse, beam diameter of 10 mm (flat-top)]. The pulsed excitation is characterized by the exposure $Q=I_p t=E_p/A$, where I_p denotes the intensity and E_p the energy of the pulse, t is the irradiation time, and A is the irradiated area. The light-induced absorption changes are probed by diode lasers of wavelengths $\lambda_t=635 \text{ nm}$ and 785 nm and a He-Ne laser at 633 nm . Fast Si diodes connected to a digital oscilloscope with an overall bandwidth of 2 GHz allow us to measure the time evolution of the transmitted light intensity $I(t)$ at a time resolution of 500 ps. The light-induced absorption is determined via

$$\alpha_{li}(t) = \frac{1}{d} \ln \left(\frac{I(t=0)}{I(t)} \right), \quad (1)$$

where d is the thickness of the crystal (solution) and $I(t=0)$ is the transmitted light intensity before the laser pulse hits the sample. Note that the crystal thickness is a mean value with respect to the penetration depth of the pump intensity. At a crystal thickness of $d=80 \mu\text{m}$ about 53% of the incoming light intensity reaches the back side of the crystal. For solutions $\alpha_{li}(t)$ is proportional to the molar light-induced extinction coefficient ϵ_{li}

$$\alpha_{li}(t) = c \epsilon_{li}(t), \quad (2)$$

where c is the molar concentration of the solution. We start the evaluation of the measured spectra at 6 ns after the trigger pulse ($t=0$), since after this time the whole pulse has passed through the crystal, and the buildup of the light-induced absorption is finished.

III. EXPERIMENTAL RESULTS

Figure 1 shows the temporal decay of a light-induced metastable state after excitation with a pump pulse [λ_p

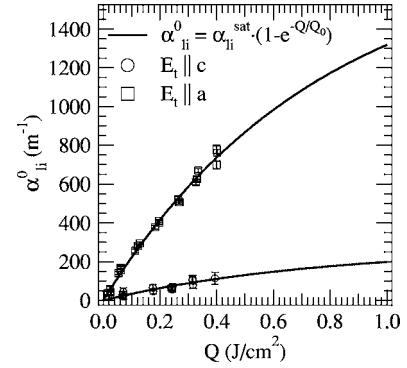


FIG. 2. Amplitude of the light-induced absorption α_{li}^0 as a function of exposure Q for two polarization directions of the probe beam ($\lambda_p=532 \text{ nm}$, $\mathbf{E}_p \parallel a, c$). The solid lines are fits using Eq. (4) yielding $\alpha_{li}^{sat}=1.8(3) \times 10^3 \text{ m}^{-1}$, $Q_0=0.8(2) \text{ J/cm}^2$ for $\mathbf{E}_t \parallel a$ and $\alpha_{li}^{sat}=0.27(2) \times 10^3 \text{ m}^{-1}$, $Q_0=0.8(3) \text{ J/cm}^2$ for $\mathbf{E}_t \parallel c$.

$=532 \text{ nm}$, $\mathbf{E}_p \parallel c$, exposure $Q=0.12(1) \text{ J/cm}^2$]. The time evolution of the light-induced absorption $\alpha_{li}(t)$ is plotted on a logarithmic time scale from $4 \times 10^{-9} - 1 \times 10^{-3} \text{ s}$ for two polarizations of the probe beam at $\lambda_t=633 \text{ nm}$ ($\mathbf{E}_t \parallel a$ in a b cut of thickness $115 \mu\text{m}$ and $\mathbf{E}_t \parallel b$ in an a cut of thickness $130 \mu\text{m}$). Independent of the pump or probe polarization direction, the decay of $\alpha_{li}(t)$ is monoexponential. The open circles and squares are the thinned datapoints and the solid line corresponds to a fit of

$$\alpha_{li}(t) = \alpha_{li}^0 \exp(-t/\tau), \quad (3)$$

where τ is the relaxation time (lifetime) and α_{li}^0 is the amplitude of the light-induced absorption at $t=0$. One observes $\tau_a=1.7(1) \times 10^{-7} \text{ s}$ and $\alpha_{li}^0=382(5) \text{ m}^{-1}$ for $\mathbf{E}_t \parallel a$ and $\tau_b=1.9(1) \times 10^{-7} \text{ s}$ and $\alpha_{li}^0=296(5) \text{ m}^{-1}$ for $\mathbf{E}_t \parallel b$. At the probing wavelength $\lambda_t=785 \text{ nm}$ the amplitudes $\alpha_{li}^0=226(10) \text{ m}^{-1}$ and $\alpha_{li}^0=181(10) \text{ m}^{-1}$ are observed for $\mathbf{E}_t \parallel a$ and $\mathbf{E}_t \parallel b$, respectively. We note that only one decay is observed and that within our time resolution (pulse width of 4 ns) the light-induced absorption occurs instantaneously, i.e., we observe only the increase of α_{li} with the laser pulse. Consequently the real generation of the metastable state is faster than 1 ns.

In order to determine the concentration of transferred molecules (population of the metastable state), we measured the light-induced absorption $\alpha_{li}(t)$ in SNP as a function of exposure Q . Figure 2 shows exemplarily the Q dependence of the amplitude α_{li}^0 for the polarization directions $\mathbf{E}_t \parallel a, c$ of the probe beam in a b cut of SNP ($\lambda_t=633 \text{ nm}$, $T=302 \text{ K}$, $d=115 \mu\text{m}$). The observed saturation behavior can be described by

$$\alpha_{li}^0(Q) = \alpha_{li}^{sat} [1 - \exp(-Q/Q_0)], \quad (4)$$

where Q_0 is the characteristic exposure needed to achieve a certain amount of population of the metastable state and α_{li}^{sat} is the saturation amplitude, which is proportional to the population, as known from absorption spectroscopy.¹⁶ One obtains $\alpha_{li}^{sat}=1.8(3) \times 10^3 \text{ m}^{-1}$ and $Q_0=0.8(2) \text{ J/cm}^2$ for $\mathbf{E}_p \parallel c$ and $\mathbf{E}_t \parallel a$. For the configuration with $\mathbf{E}_p \parallel c$ and $\mathbf{E}_t \parallel c$ the

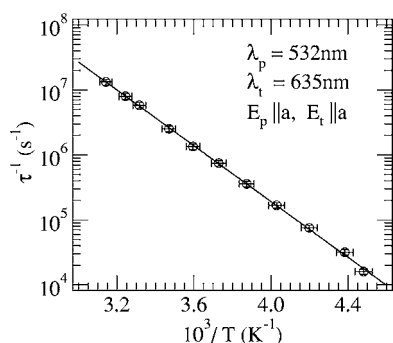


FIG. 3. Arrhenius plot of the relaxation times in SNP for polarization of the pump and probe beams parallel to the a axis of the crystal (b cut, $d=760 \mu\text{m}$). The fit (solid line) yields an activation energy of $E_A=0.43(3)$ eV and a frequency factor of $Z=7(3) \times 10^{13} \text{ s}^{-1}$.

saturation amplitude is about six times smaller $\alpha_{li}^{sat} = 0.27(2) \times 10^3 \text{ m}^{-1}$, whereas $Q_0=0.8(3) \text{ J/cm}^2$ remains the same within errors.

From the temperature dependence of the relaxation time τ of the monoexponential decay the activation energy E_A and the frequency factor Z are obtained via the Arrhenius relation

$$\tau = \frac{1}{Z} \exp\left(\frac{E_A}{k_B T}\right). \quad (5)$$

Figure 3 shows the findings for $E_p \parallel a$ and $E_t \parallel a$ ($\lambda_t=635$ nm), yielding the activation energy $E_A=0.43(3)$ eV and the frequency factor $Z=7(3) \times 10^{13} \text{ s}^{-1}$. The errors are given by the statistics of the detected data points and we note that the accuracy of Z is in the range of one order of magnitude due to the rather small temperature interval of about 100 K, where the Arrhenius behavior was detected.

In order to demonstrate the existence of the light-induced metastable state in liquids, we have detected the transient kinetics of the light-induced absorption as a function of the concentration c of aqueous solutions of SNP. Figure 4 shows the amplitude of the light-induced absorption of the solution at the pulse energy 85 mJ ($\lambda_p=532$ nm, $\lambda_t=633$ nm, T

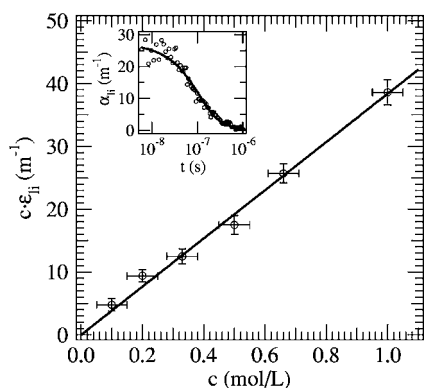


FIG. 4. Amplitude of the light-induced absorption at $\lambda_t=633$ nm in aqueous solutions of SNP for different concentrations at a pulse energy of 85 mJ. The insert shows the monoexponential decay with $\tau=1.1(1) \times 10^{-7} \text{ s}$ for a 0.66 molar solution of SNP.

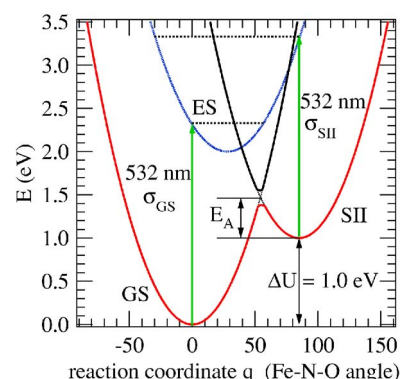


FIG. 5. (Color online) Potential scheme for generation and relaxation of SII in SNP.

$=300$ K). The slope $\epsilon_{li}=38(1) \text{ m}^{-1} \text{ L mol}^{-1}$ of the linear increase as a function of the concentration corresponds to the molar light-induced extinction coefficient at $\lambda_t=633$ nm [Eq. (2)]. The inset in Fig. 4 shows the temporal decay after the single pulse excitation for a pulse energy of 85 mJ and a concentration of 0.66 mol L^{-1} . The lifetime of the monoexponential decay is $\tau=1.1(1) \times 10^{-7} \text{ s}$, slightly shorter than the lifetimes $\tau_{a,b}$ observed in the single crystals.

IV. DISCUSSION

The observed light-induced absorption changes can be attributed to the metastable state SII in SNP due to the following reasons: (i) The activation energy $E_A=0.46(3)$ eV and frequency factor $Z=1 \times 10^{14} \text{ s}^{-1}$ known from DSC measurements at low temperatures (130–150 K)¹⁵ correspond well with the values $E_A=0.43(3)$ eV and $Z=7(3) \times 10^{13} \text{ s}^{-1}$ determined from the temperature dependence of the relaxation time τ in the temperature range 220–320 K, indicating that E_A and Z are independent of temperature. (ii) The polarization dependence of the amplitude α_{li}^0 of the light-induced absorption shows the same behavior as found for steady-state polarized absorption spectroscopy,¹⁶ where also a six times stronger absorption was observed for the polarization of the probe beam parallel to the a axis compared to the c axis at 633 nm (Fig. 9 in Ref. 16). (iii) The amplitude of the light-induced absorption α_{li}^0 is larger at $\lambda_t=633$ nm than at $\lambda_t=785$ nm, i.e., α_{li}^0 decreases with increasing probing wavelength. This agrees also with the results of (Ref. 16), where the absorption maximum of SII was found at about 640 nm. For SI the maximum of the absorption band is at about 780 nm and hence the larger amplitude α_{li}^0 should occur at $\lambda_t=785$ nm compared to $\lambda_t=633$ nm.

Following the results of x-ray and neutron diffraction,^{18,20} DFT calculations,²⁴ and the proposals in Refs. 16 with respect to the absorption spectroscopic results the generation of SII at room temperature can be explained according to Fig. 5 in the following way: With short laser pulses an excitation from the ground state (GS) (1A_1) into the intermediate excited state (ES) occurs and from there a relaxation into SII takes place. This electronic rearrangement is connected with the structural change of the NO ligand, the rotation from the

nearly linear Fe-N-O bond to the nearly 90° *side-on* position of the NO ligand (reaction coordinate q =Fe-N-O angle). Because of the very short lifetime ($\tau < 4 \times 10^{-9}$ s) in the excited state (ES) [corresponds to $\pi^*(\text{NO})$ in the orbital picture] we can conclude that a singlet state and not a triplet state is generated in this intermediate state so that the diamagnetic spin configuration $S=0$ is conserved in GS, ES, and SII. Hence ES is a degenerate 1E state. The degeneracy is lifted due to the Jahn-Teller interaction via vibrational e -modes, e.g., the deformation vibration $\delta(\text{Fe-N-O})$. A more detailed analysis of such a 1E Jahn-Teller coupling mechanism leading to the photoisomerization has been given in a recent DFT study.²⁵ This means in the potential scheme of Fig. 5 that the potential curves of ES and SII meet at the crossing point at about $q=45^\circ$, where the excited electron can relax into the SII basin, thereby forming the long-lived 1A_1 ground state in the SII configuration at sufficiently low temperatures. As known from Mössbauer and DSC measurements this SII 1A_1 state is about 1 eV above the GS 1A_1 . However, at room temperature due to the frequency factor of $Z=7 \times 10^{13} \text{ s}^{-1}$ and the potential well of 0.43 eV the metastable state SII returns thermally driven back into GS via the crossing point between GS and SII at about $q=55^\circ$.

Using the results illustrated in Fig. 2 we can calculate the population of SII in saturation and indicate an upper bound for the population of SI. From low-temperature absorption spectroscopy¹⁶ the absorption coefficients for GS, SII, and SI are known. For polarization $E \parallel a$ the absorption coefficient α at $\lambda=633$ nm has the values $\alpha^{\parallel a}(\text{SII})=2200 \text{ cm}^{-1}$ for SII and $\alpha^{\parallel a}(\text{SI})=83 \text{ cm}^{-1}$ for SI. Using $\alpha_{ii}^{\text{sat}}=18 \text{ cm}^{-1}$ from Fig. 2 we obtain a population of $P(\text{SII})=0.8\%$ in saturation. Hence we achieve a population of 0.4% at our maximal exposure of 0.4 J/cm^2 . Within our sensitivity of 0.05 cm^{-1} we were not able to detect the decay of the metastable state SI at the different probing wavelengths. Hence we can indicate an upper bound of $P(\text{SI})=0.03\%$ for the obtainable population for SI in our pump configuration, when considering the probe wavelength $\lambda_i=785$ nm, where SI exhibits an absorption band with $\alpha^{\parallel a}(\text{SI})=155 \text{ cm}^{-1}$.¹⁶ Furthermore this indicates that SII thermally does not decay into SI and therefore the potential barrier between SII and SI is significantly higher than that between SII and GS (0.43 eV). As indicated in Fig. 5 the saturation population of SII at 532 nm is determined by the ratio of the cross sections $\sigma_{\text{GS}}/\sigma_{\text{SII}}$,

$$\frac{\alpha_{\text{GS}}}{\alpha_{\text{SII}}} = \frac{n_{\text{GS}} \cdot \sigma_{\text{GS}}}{n_{\text{SII}} \cdot \sigma_{\text{SII}}}, \quad (6)$$

where $\alpha_{\text{GS,SII}}$ are the absorption coefficients for GS and SII and $n_{\text{GS,SII}}$ denotes number densities of molecules in GS and SII. The ratio $n_{\text{GS}}/n_{\text{SII}}=124$ is known from the population of SII of 0.8%, while the ratio $\alpha_{\text{GS}}/\alpha_{\text{SII}}=0.154$ at 532 nm is known from absorption spectroscopy.¹⁶ Hence we can determine $\sigma_{\text{GS}}/\sigma_{\text{SII}}=1.25 \times 10^{-3}$ for $\lambda_p=532$ nm.

The results of the pulsed generation of the metastable states are in good agreement with the conclusions of a wavelength and temperature dependent study of the population

dynamics using continuous wave (cw) illumination.²⁶ The observed population of SII generated by 532 nm nanosecond pulses is consistent with the saturation population obtained by cw illumination with 530.9 nm,²⁶ where also less than 1% SII were obtained directly. The temperature dependent measurements of the population degree of SI in Ref. 26 show a gradual decrease of the obtainable SI population from 20% at 140 K to far less than 1% at 160 K for cw illumination with 530.9 nm. In Ref. 26 it was also shown that the population of SI is possible up to 200 K using cw illumination with 457.9 nm. Above 200 K the decay rate of SI is of the order of the generation rate and therefore steady-state measurements are no longer suitable for investigation of the population process of SI. The authors of this extensive study concluded that in the green-yellow spectral range the generation of SI occurs via SII, i.e., $\text{GS} \rightarrow \text{SII} \rightarrow \text{SI}$, while in the blue spectral range a direct generation $\text{GS} \rightarrow \text{SI}$ is additionally possible. Hence the fact that we do not observe a significant population of SI ($\leq 0.03\%$) when illuminating with 532 nm at room temperature is in complete agreement with these findings. Furthermore we would expect that the generation of SI at room temperature is possible using short laser pulses in the blue-violet spectral range.

In view of potential biological or medical applications based on the metastable states it is necessary to generate them also in solution. Figure 4 shows the transient kinetics of the light-induced absorption as a function of the concentration c of aqueous solutions of SNP. The lifetime τ of SII at $T=300$ K is $1.1(1) \times 10^{-7}$ s, slightly shorter than in the solid state, indicating that the environment of the $[\text{Fe}(\text{CN})_5\text{NO}]^{2-}$ anion has considerable influence on the lifetime of SII. Hence SII can be generated by pulsed illumination in solutions and SI is generated by cw illumination in cooled liquids,¹⁴ which means that we need only the $[\text{Fe}(\text{CN})_5\text{NO}]^{2-}$ anion as a carrier. In order to reach a sufficiently long lifetime at $T=37^\circ\text{C}$ compounds with Ru as the central atom are promising candidates.⁸

V. CONCLUSION

Using nanosecond pulses at $\lambda=532$ nm the metastable state SII can be generated at $T=300$ K exhibiting a lifetime of $1.8(1) \times 10^{-7}$ s for single crystals and $1.1(1) \times 10^{-7}$ s for aqueous solutions of SNP. Consequently the use of the metastable states in photonic or biological applications at room temperature is feasible. The generation of SII, i.e., the rotation of the NO ligand by about 90°, is faster than 1 ns and hence occurs via a singlet excited state. Using femtosecond pulses one should therefore be able to observe the rotation of the NO ligand.

ACKNOWLEDGMENTS

Financial support by the Swiss National Science Foundation (Grant No. PBEZ2-100873) and the Deutsche Forschungsgemeinschaft (Grant Nos. WO618/5-3, IM37/2-1) is gratefully acknowledged.

- *Electronic address: dominik.schaniel@uni-koeln.de
- ¹M. Imlau, S. Odulov, T. Bieringer, and Th. Woike, in *Nanoelectronics and Information Technology*, edited by R. Waser (Wiley-VCH, Weinheim, 2003), p. 659.
- ²M. Imlau, S. Haussühl, Th. Woike, R. Schieder, V. Angelov, R. A. Rupp, and K. Schwarz, *Appl. Phys. B* **68**, 877 (1999).
- ³E. Culotta and D. E. Koshland, *Science* **258**, 1862 (1992).
- ⁴J. S. Stamler, D. J. Singel, and J. Loscalzo, *Science* **258**, 1898 (1992).
- ⁵L. Ignarro and F. Murad, *Nitric Oxide: Biochemistry, Molecular Biology, and Therapeutic Implications*, Advances in Pharmacology, Vol. 34 (Academic, New York, 1995).
- ⁶*Nitric Oxide: Principles and Actions*, edited by J. Lancaster, Jr. (Academic, San Diego, 1996).
- ⁷L. Cheng and G. B. Richter-Addo, *The Porphyrin Handbook*, edited by K. M. Kadish, K. Smith, and R. Guilard (Academic, San Diego, 2000), Vol. 4, p. 219.
- ⁸D. Schaniel, Th. Woike, B. Delley, C. Boskovic, D. Biner, K. Krämer, and H. U. Güdel, *Phys. Chem. Chem. Phys.* **7**, 1164 (2005).
- ⁹U. Hauser, V. Oestreich, and H. D. Rohrweck, *Z. Phys. A* **280**, 17 (1977).
- ¹⁰Th. Woike, M. Imlau, V. Angelov, J. Schefer, and B. Delley, *Phys. Rev. B* **61**, 12249 (2000).
- ¹¹Th. Woike and S. Haussühl, *Solid State Commun.* **86**, 333 (1993).
- ¹²J. A. Guida, O. E. Piro, and P. J. Aymonino, *Inorg. Chem.* **34**, 4113 (1995).
- ¹³Y. Morioka, A. Ishikawa, H. Tomizawa, and E. Miki, *J. Chem. Soc. Dalton Trans.* **5**, 781 (2000).
- ¹⁴H. Zöllner, W. Krasser, Th. Woike, and S. Haussühl, *Chem. Phys. Lett.* **161**, 497 (1989).
- ¹⁵D. Schaniel, Th. Woike, L. Tsankov, and M. Imlau, *Thermochim. Acta* **429**, 19 (2005).
- ¹⁶D. Schaniel, J. Schefer, B. Delley, M. Imlau, and Th. Woike, *Phys. Rev. B* **66**, 085103 (2002).
- ¹⁷M. Imlau, Th. Woike, R. Schieder, and R. A. Rupp, *Phys. Rev. Lett.* **82**, 2860 (1999).
- ¹⁸M. D. Carducci, M. R. Pressprich, and P. Coppens, *J. Am. Chem. Soc.* **119**, 2669 (1997).
- ¹⁹D. Schaniel, J. Schefer, M. Imlau, and Th. Woike, *Phys. Rev. B* **68**, 104108 (2003).
- ²⁰D. Schaniel, Th. Woike, J. Schefer, and V. Petricek, *Phys. Rev. B* **71**, 174112 (2005).
- ²¹M. Kawano, A. Ishikawa, Y. Morioka, H. Tomizawa, E. Miki, and Y. Ohashi, *J. Chem. Soc. Dalton Trans.* **14**, 2425 (2000).
- ²²P. Coppens, I. Novozhilova, and A. Kovalevsky, *Chem. Rev. (Washington, D.C.)* **102**, 861 (2002).
- ²³K. Ookubo, Y. Morioka, H. Tomizawa, and E. Miki, *J. Mol. Struct.* **379**, 241 (1996).
- ²⁴B. Delley, J. Schefer, and Th. Woike, *J. Chem. Phys.* **107**, 10067 (1997).
- ²⁵M. Atanasov and T. Schönherr, *J. Mol. Struct.* **592**, 79 (2002).
- ²⁶Th. Woike, W. Krasser, H. Zöllner, W. Kirchner, and S. Haussühl, *Z. Phys. D: At., Mol. Clusters* **25**, 351 (1993).